Electronic Supplementary Material (ESI) for Catalysis Science & Technology.

Supporting Information

Understanding the Entropic Effect in Chorismate Mutase Reaction Catalyzed by Isochorismate-Pyruvate Lyase from *Pseudomonas Aeruginosa* (PchB)

Liangxu Xie[1,3], Mingjun Yang[2]*, Zhe-Ning Chen[1]*

[1] State Key Laboratory of Structural Chemistry, Fujian Institute of Research on the Structure of Matter, Chinese Academy of Sciences, 155 Yangqiao Road West, Fuzhou 350002, China.

[2] XtalPi Inc.,Times Science & Tech Mansion E. 20F, 7028 Shennan Ave, Futian District, Shenzhen, China

[3] Department of Chemistry, The University of Hong Kong, Pokfulam Road, Hong Kong S. A. R., China.

*Email: znchen@fjirsm.ac.cn (Z. -N. Chen); mjyang2011@gmail.com (M. -J. Yang)

Scheme S1. Schematic figure illustrating the rearrangement of chorismate into prephenate. The dihedral values of chorimsate are shown as black and red in water and in PchB, rescpectively

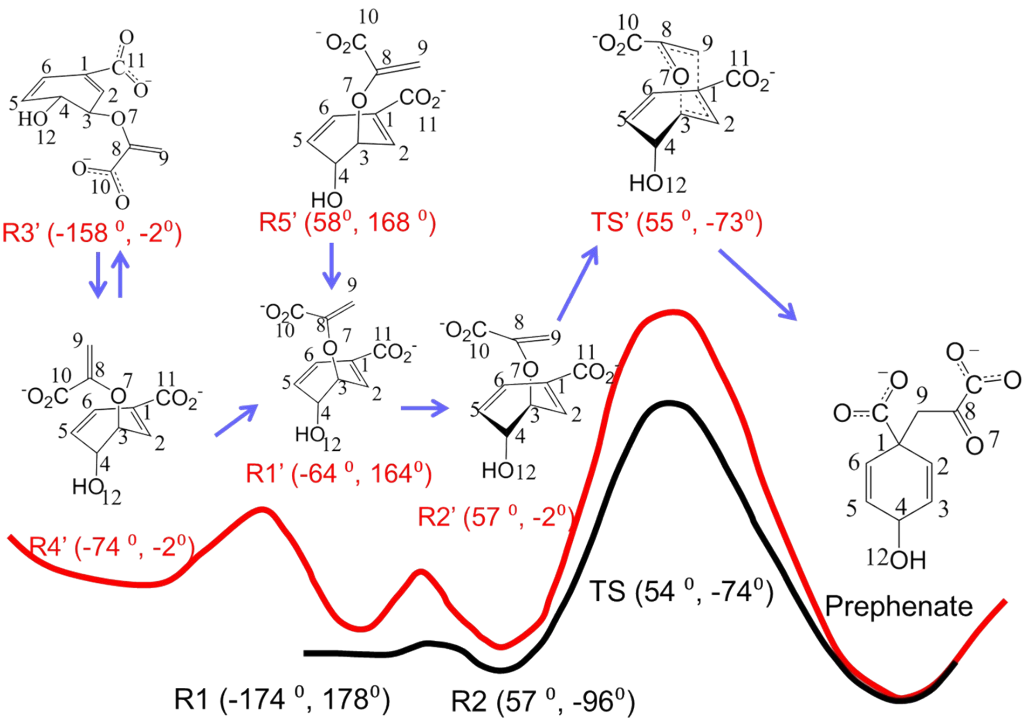

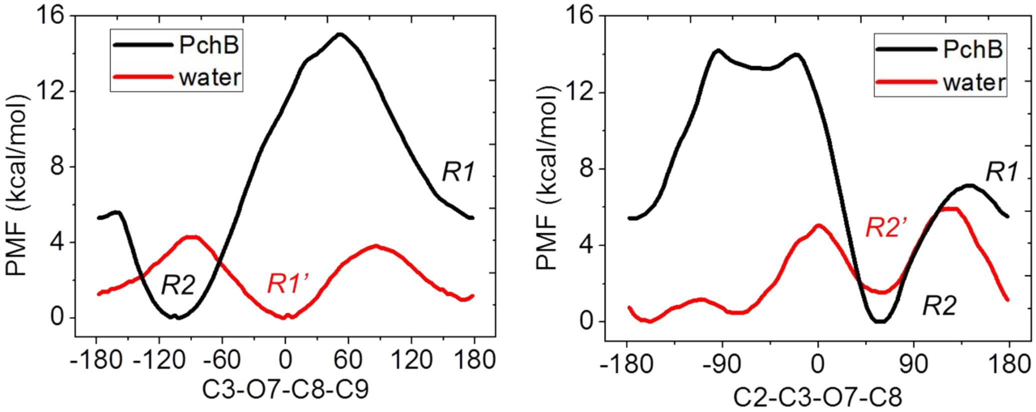

Fig. S1 Free energy profile of chorismate at groupd state. 1-D PMF plot for chorismate in PchB and in water as a function of dihedral C2–C3–O7–C8 and C3–O7–C8–C9 which obtains from US sampling at DFTB2/MIO/MM level. Local minima are labeled as are labeled as state R1 and R2 in PchB, and R1’ and R2’ in water.

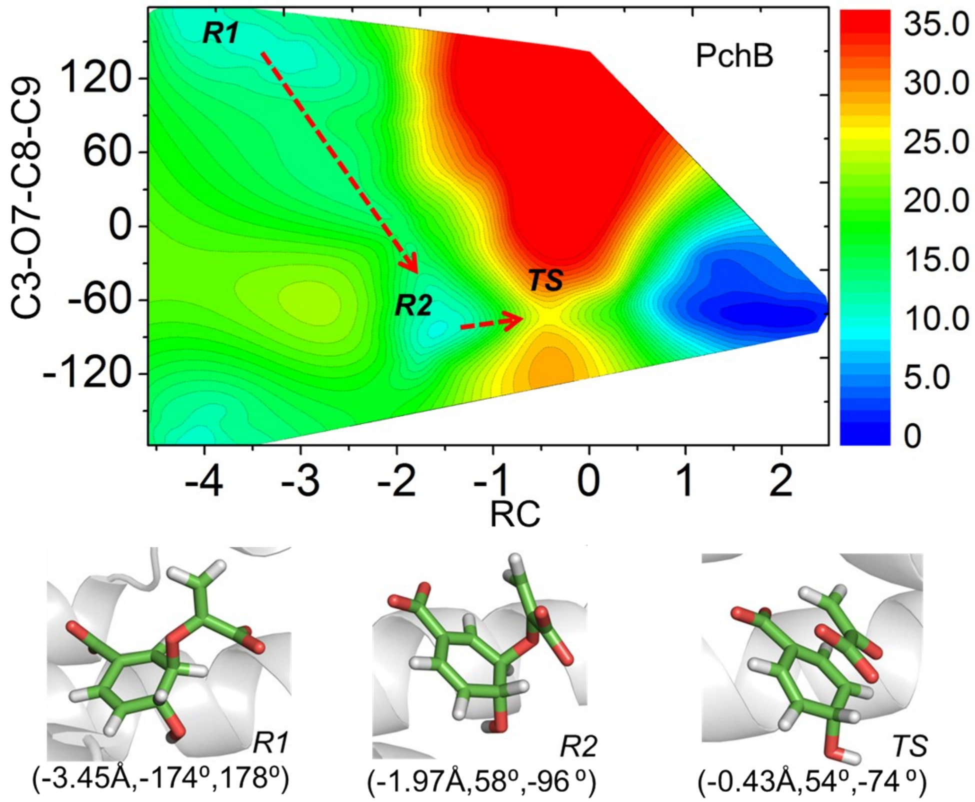

Fig. S2 PMF profiles of PchB catalyzed reaction. PMF profiles as the reaction coordinates of dihedral C3-O7-C8-C9 and the chemical reaction coordinate RC in PchB. MD snapshots of each state for chorismate in PchB. RC is defined as the antisymmetric combination of the breaking and forming bonds, $d_{C3\text{-}O7}\text{-}d_{C1\text{-}C9}$. The minimum free energy paths were labeled with arrows on the figure. The RC, dihedral values of C2-C3-O7-C8 and C3-O7-C8-C9 are labeled for each representative structure.

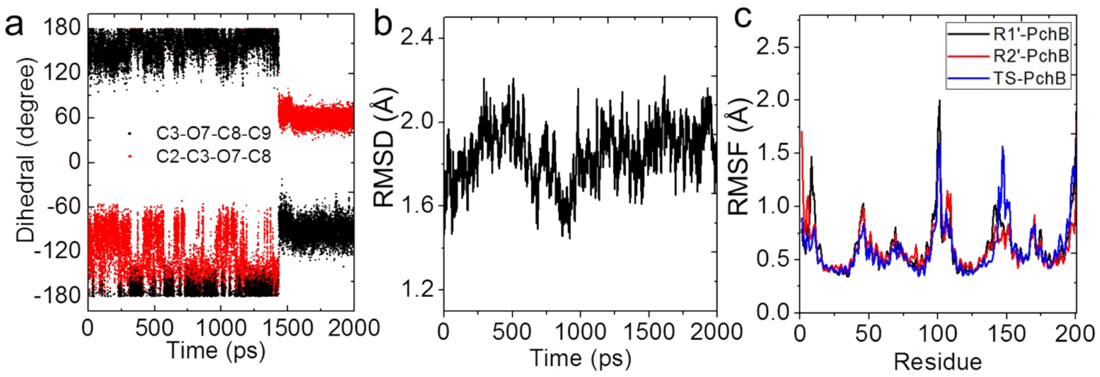

Fig. S3 Structural changes during MD simulations. (a) The dihedral change propagation of chorismate in PchB starting from state R1'; (b) Root mean square deviation (RMSD) change; and (c) Root mean square fluctuation (RMSF) for the trajectory obtained by using the local minimum as the initial structure in the 2000ps QM/MM MD simulations.

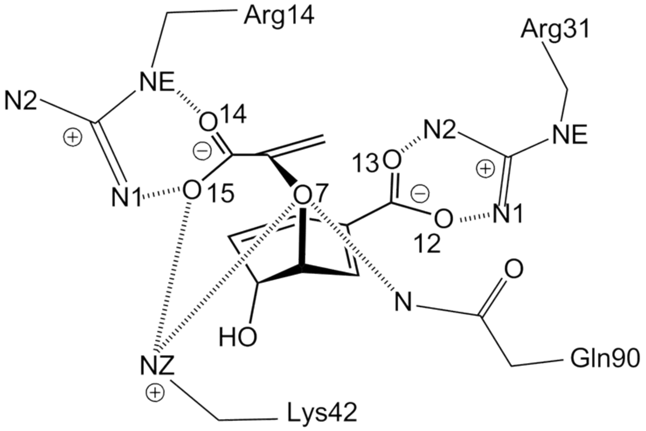

Fig. S4 Schematic of electrostatic interactions between chorismate and PchB residues. Hydrogen atoms have been removed for clarity. Average distances are shown in Table S2.

Tables

Table S1. Simulation details for conformational transformation and chemical reaction steps.

Simulation type	**system**	**Method**[a]	**Reaction coordinates**	**Simulation time**[b]	**T (K)**
Dihedral scanning with 2D US	water	DFTB2/MIO/MM	Dihedral C3–O7–C8–C9 and C2–C3–O7–C8	64.8 ns (50ps × 1296 windows)	298
	PchB			30 ns (50ps × 600 windows)	
Reaction path with 1D US	water	DFTB2/MIO/MM	$d_{(\mathrm{C3\text{-}O7})} - d_{(\mathrm{C1\text{-}C9})}$	9.9 ns (100ps × 99 windows)	298
	PchB			10.8 ns (100ps × 108 windows)	
Free energy calculation	water	DFT/MM	$d_{(\mathrm{C3\text{-}O7})} - d_{(\mathrm{C1\text{-}C9})}$	0.54 ns (20ps × 27 windows)	298
	PchB				
Entropy calculation	water	DFTB2/MIO/MM	$d_{(\mathrm{C3\text{-}O7})} - d_{(\mathrm{C1\text{-}C9})}$	980 ns (1ns × 49 windows × 20 replicas)	278, 288, 298, 308, 318
	PchB				293, 298, 303, 308,

					313

[a] In all these simulations, the substrate molecule was treated by DFT or DFTB2/MIO method and the remaining protein and water molecules were treated by CHARMM force field.

[b] The simulation time for each window and the number of windows are listed in the parentheses. The simulation is same unless stated otherwise.

Table S2. Average distances (in units of Å) between enzyme residues and chorismate.

chorismate–residue	PchB–*R1*	PchB–*R2*	PchB–*TS*
O12-N1~Arg31	3.33	2.68	2.66
O13-N2~Arg31	3.63	2.74	2.76
O14-NE~Arg14(B)	3.56	2.70	2.72
O15-N1~Arg14(B)	4.71	2.69	2.66
O15-NZ~Lys42	2.85	2.68	2.71
O7-NZ~Lys42	5.57	3.12	2.99
O7-N~Gln90	4.60	2.98	2.92
C9-CZ~Arg14(B)	4.44	3.94	3.95
C9-NZ~Lys42	3.20	3.64	3.65

Selected distances for chorismate and the closest residues of the enzyme are summarized in Table 3. An obvious difference between *R2* and *TS* is the decrease in distance between ether oxygen (O7) and neighboring residues. In the *TS*, the broken C3–O7 bond is stabilized by stronger electrostatic interactions. The O7–NZ~Lys42 distance decreases from 3.12 to 2.99 Å, as well as the O7–N~Gln90 distance decreases from 2.98 to 2.92 Å. Lys42 and Gln90 establish a strong hydrogen bond and electrostatic stabilization with ether oxygen O7. Among them, O7–

NZ~Lys42 shows the largest distance change when *R2* converts into *TS*.

Table S3. Free energy (kcal/mol), decomposed enthalpy and entropy (in cal/mol/K) for the reaction in PchB and in water.

	Exp		**DFTB2/MIO**		**DFT**	**AM1**
	$\Delta G^{\ddagger}$	**$\Delta S^{\ddagger}$**	**$\Delta G^{\ddagger}$**	**$\Delta S^{\ddagger}$**	**$\Delta G^{\ddagger}$**	**$\Delta G^{\ddagger}$**
Water	24.5 [a]	-12.9	15.6 ± 0.24	-8.6	22.0	29.3 [c]
PchB	19.5 [b]	-12.1	12.1 ± 0.10	-3.4 (-10.5)[d]	17.3	27.0 [c]

[a] experimental values are taken from ref [1].

[b] experimental values are taken from ref[2].

[c] Theoretical values calculated at AM1 level are taken from ref[3].

[d] The entropy value includes the entropy change from pre-organization step (-10.5 cal/mol/K) and chemical reaction step (-3.4 cal/mol/K.)

Table S4. Key distance (in units of Å) and dihedral changes (in units of degree) for reactions in water and in PchB averaged from DFTB2/MIO/MM simulations.

	PchB		**water**	
	R2	*TS*	*R2'*	*TS'*
RC	−1.97	−0.43	−2.11	−0.45
$d_{C3\text{-}O7}$	1.51	1.91	1.49	1.85
$d_{C1\text{-}C9}$	3.48	2.34	3.60	2.30
$d_{C10\text{-}C11}$	5.23	4.73	6.48	4.84
C2-C3-O7-C8	57.9	53.9	57.4	54.9
C3-O7-C8-C9	−95.7	−74.3	−1.9	−73.1

Table S5. Entropy change during conformation conversion process and chemical reaction process. Entropy is in the unit of cal/mol/K.

	transformation	**reaction**	**overall**
ΔS_{QHA}	− 10.5	− 5.8	− 16.3
ΔS_{CAP} [a]	−	− 3.4	− 13.9 [b]

[a] using least-square fitting of Computational Arrhenius plot; [b] using transformation entropy in the first column for transformation step.

References

1. P. R. Andrews, G. D. Smith and I. G. Young, *Biochemistry*, 1973, **12**, 3492-3498.

2. Q. Luo, K. M. Meneely and A. L. Lamb, *J. Am. Chem. Soc.*, 2011, **133**, 7229-7233.

3. S. Martí, J. Andrés, V. Moliner, E. Silla, I. Tuñón, J. Bertrán and M. J. Field, *J. Am. Chem. Soc.*, 2001, **123**, 1709-1712.